Hindawi
Advances in Civil Engineering
Volume 2020, Article ID 3541329, 6 pages
https://doi.org/10.1155/2020/3541329

Research Article

Formulation of a Yield Surface for Sand Based on the Elastic Threshold Strain

Sang Inn Woo

Department of Civil and Environmental Engineering, Hannam University, 70 Hannam-ro, Daejeon 34430, Republic of Korea

Correspondence should be addressed to Sang Inn Woo; sanginnwoo@gmail.com

Received 8 October 2019; Revised 21 February 2020; Accepted 19 March 2020; Published 11 April 2020

Academic Editor: Jian Ji

The present study proposes a rigorous expression of a yield function for sand based on the linear elastic threshold strain concept and empirical expression for the maximum shear modulus. The new yield function was calibrated for Toyoura sand. The calibration results show that the proposed yield surfaces are nonlinear curves that depend on the void ratio of sand in the p'-q plane, whereas the linear lines have been adopted in the bounding surface modeling of sand. This study also found that elliptic yield surfaces are the best fitted with the proposed yield surface and they can be used as alternatives to the proposed yield surface under the undrained shearing where the void ratio (or density) of sand is fixed.

1. Introduction

Bounding surface models [1–7] have successfully described mechanical responses of sand including highly nonlinear stress-strain relationship [8–11], entrance to the critical state upon prolonged shearing [10–13], and dilatancy [10, 14–18], which is plastic volumetric deformation caused by plastic shear deformation. Figure 1 shows the bounding, critical-state, and yield surfaces that have been commonly applied in the bounding surface models [1–7] in the p-q' (where p' is mean effective stress ($=\sigma'_{kk}/3$), q is von Mises stress $=((3/2)\, s_{ij}s_{ij})$, and σ'_{ij} is the effective stress ($=\sigma_{ij}-u\delta_{ij}$), u is pore-water pressure, and s_{ij} is deviatoric stress ($=\sigma_{ij}-(\sigma_{kk}/3)\ \delta_{ij}$)) plane where those surfaces are expressed as linear lines of which slopes are M_b, M_c, and m, respectively, under the isotropic consolidation conditions. In Figure 1, the critical-state surface is the final destination of the stress upon shearing; the bounding surface corresponds to the peaks which depend on the density (or void ratio) of sand and confining pressure acting on sand; the yield surface is a region where sand shows elastic responses.

To calibrate the critical state surface, the bounding surface models [1–7] relies on the final stress state (e.g., final values of p' and q) of sand upon shearing after full stabilization of stress was confirmed; then, they calculated the critical state stress ratio M_c ($=(q/p')_c$ (where subscript c denotes the critical state)) using the stress at the critical state; thus, this calibration step is quite straightforward. For the calibration of the bounding surface (which corresponds to the peak), the pairs (e, p') of the void ratio and mean effective stress at the peaks are used to calculate the values of the state parameter ψ [19] (which is defined as a vertical distance to the critical state line from the current (e, p') state in the e-p' space) for numerous shearing tests; after this step, the slope M_b of the bounding surface can be expressed as a function of the state parameter ψ; thus, the calibration of the bounding surface relies on the quantitative manner. For the yield surface, the previous research studies on the bounding surface modeling for sand [1–7] have tried to reflect the fact that the elastic region of sand is very small in the stress space. The authors in [1, 2, 4] set the $m = 0.05$ in their models, whereas Dafalias and Manzari [5] used a yield surface with $m = 0.01$; some bounding surface models [3, 6, 7] even relied on the yield line (so, the slope m of a yield surface is zero) so that there is no elastic region in their models. For these bounding surface models, however, the determination of the yield surface has not followed the calibration step using experimental data in a quantitative manner. From this background, the following concern arises: "Is the linear line enough to express the elastic range of sand in the stress

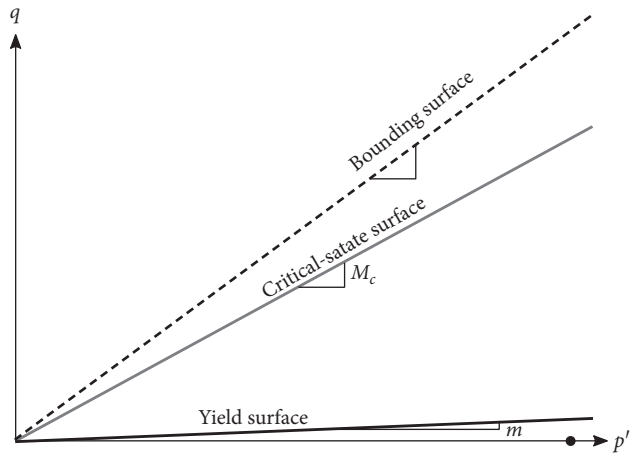

Figure 1: Bounding, critical-state, and yield surfaces for isotropically consolidated sand samples in the p'-q plane used in the bounding surface models [1, 2, 5].

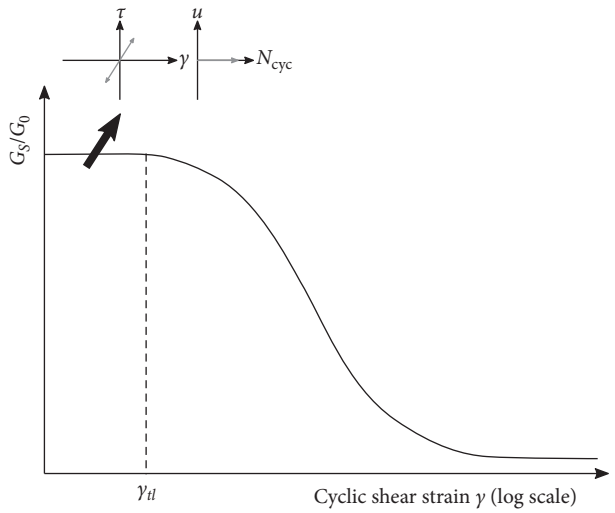

Figure 2: Typical degradation curve of secant shear modulus G_s to cyclic shear strain γ and definition of the linear elastic threshold strain γ_{tl} during undrained cyclic shearing.

space?". This study deals with this concern using the elastic threshold strain concept.

Figure 2 shows the typical degradation curve of the ratio between the secant shear modulus G_s and maximum shear modulus G_0 under the undrained cyclic shearing. In Figure 2, if the cyclic shear strain γ is less than the linear elastic threshold strain γ_{tl}, the sand shows the linear elastic response and there is no plastic dissipation; therefore, the linear elastic threshold strain represents the elastic range in the strain field and it should correspond to the yield surface in the stress space. Although Figure 2 represents the undrained response, this degradation is valid also under the drained conditions until the shear strain is less than the volumetric (or cyclic) threshold strain, which is much greater than the linear elastic threshold strain γ_{tl}, because there is no dilatancy before the strain reaches the volumetric threshold strain. Based on this, this study aims to propose the new yield surface (or yield function) using the concept of the elastic threshold strain.

2. Formulation

According to Hardin and Richart [20], the maximum shear modulus G_0 is a function of void ratio e and mean effective stress p':

$$G_0 = C_g \frac{\left(e_g - e\right)^2}{1+e} p_A^{1-n_g} p'^{n_g}, \tag{1}$$

where p_A is the reference pressure (=100 kPa) and C_g, e_g, and n_g are positive material parameters. Equation (1) implies that G_0 has the greater value as e is the less or p' is the greater. If the shear strain is less than the elastic threshold strain, the sand shows the linear elastic response (Figure 2); in this case, under the pure shear loading conditions after the isotropic consolidation, the relationship between shear stress τ and (engineering) shear strain γ is written by

$$\tau = G_0 \gamma. \tag{2}$$

When shear strain γ exceeds the linear elastic threshold strain γ_{tl}, the plastic deformation starts to happen; thus, the yield shear stress τ_y can be written by

$$\tau_y = G_0 \gamma_{\mathrm{tl}}, \tag{3}$$

which represents the yield condition of sand under the pure shear loading conditions after the isotropic consolidation. Substitution of equation (1) into equation (3) leads

$$\tau_y = C_g \gamma_{\mathrm{tl}} \frac{\left(e_g - e\right)^2}{1+e} p_A^{1-n_g} p'^{n_g}. \tag{4}$$

Under the pure shear conditions (or the simple shear conditions with very small strain) after isotropic consolidation, the relationship between shear stress τ and von Mises stress q is

$$q = \sqrt{3}\tau. \tag{5}$$

After substitution of equation (5) into equation (4),

$$q_y = \left[\sqrt{3}\, C_g \gamma_{\mathrm{tl}} \frac{\left(e_g - e\right)^2}{1+e} p_A^{1-n_g}\right] p'^{n_g} = m(e) p'^{n_g}, \tag{6}$$

where q_y is the yield von Mises stress; thus, under the pure shear loading after the isotropic consolidation, the yield function of sand can be written by

$$f = q - m(e) p'^{n_g} = 0. \tag{7}$$

The bounding surface models [1–7] have considered the stress anisotropy for the critical-state and bounding surfaces; however, they have assumed the isotropic yield surface so far; for the sake of simplicity, this study also relies on the isotropic yield surface for sand and there is no dependency of the yield function on loading directions. Considering the kinematic hardening rule, the yield function in equation (7) can be extended to

$$f = |q - ap'| - m(e)p'^{n_g}, \tag{8}$$

where a is the back-stress ratio which represents the middle line of the yield surface. The gradients $\partial f/\partial q$ and $\partial f/\partial p'$ of the yield function f to q and p' are

$$\frac{\partial f}{\partial q} = \frac{(q - ap')}{\sqrt{(q - ap')(q - ap')}} = s, \tag{9}$$

$$\frac{\partial f}{\partial p'} = -sa - m(e)n_g p'^{n_g - 1}, \tag{10}$$

where variable s has 1 and -1 if $q > ap'$ and $q < ap'$, respectively. The gradient $\partial f/\partial q$ (equation (9)) of f to q has the same form with the linear line yield functions [1, 2]; however, the gradient $\partial f/\partial p'$ (equation (10)) of f to p' has an additional term (the second term in equation (10)), which makes the yield surface gradually parallel to the back-stress ratio as p' increases (as n_g is generally less than 1).

3. Calibration Yield Surface for Toyoura Sand

The construction of the yield function (equation (8)) requires the calibration of C_g, e_g, n_g, and γ_{tl} for sand. According to Bolton and Oztoprak [21], the lower bound, upper bound, and mean value of the linear elastic threshold strain γ_{tl} are 0, 3×10^{-5}, and 7×10^{-6} from 750 test data for various sands; in this study, the average value 7×10^{-6} of γ_{tl} is used for the yield surface. For Toyoura sand (clean uniform sand of which maximum and minimum void ratios are approximately 1.0 and 0.6, respectively), Woo et al. [22] and Woo and Salgado [2] calibrated C_g, e_g, and n_g as 850, 2.17, and 0.45, respectively, using a number of the resonance column, torsional shear, and bender element test results. Table 1 listed the calibrated parameters of the proposed yield surface for Toyoura sand.

Figure 3 plots the calibrated yield surfaces with the back-stress ratio $a = 0$ for Toyoura sand when void ratio $e = 0.6$, 0.7, 0.8, 0.9, and 1.0; it also draws linear yield surfaces with $m = 0.005$, 0.01, 0.02, and 0.05. In Figure 3, the proposed yield surface (developed from the linear elastic threshold strain concept and based on the experimental data) depends on the void ratio; the denser sand has the greater yield surface. Although the linear yield surfaces have been commonly used for the bounding surface models [1, 2, 4, 5], Figure 3 shows that the proposed yield surfaces are nonlinear curves in the p'-q plane. Focusing on low confinement situations ($p' < 100$ kPa), a yield surface [1, 2, 4] with $m = 0.05$ overestimates the elastic region of Toyoura sand, whereas yield surfaces [3, 5–7] with $m < 0.01$ generally underestimates the elastic region of Toyoura sand in the stress space.

4. Comparision with the Elliptic Yield Surface

Taiebat and Dafalias [23] assessed the availability of the elliptical, lemniscate, distorted lemniscate, and eight-curve functions as yield functions for soil constitutive modeling; according to Taiebat and Dafalias [23], the lemniscate, distorted lemniscate, and eight-curve yield surfaces have a sharp tip at the origin in the p'-q plane, whereas the elliptical yield surface has a smooth tip at the origin; as the proposed yield surface (Figure 3) has a smooth tip at the origin in the p'-q plane, this study selects the elliptic yield function to compare it with the proposed yield surface. In Taiebat and Dafalias [23], one of the elliptic yield functions can be written by

$$f_e = |q - ap'| - m\sqrt{p'(p_0 - p')} = 0, \tag{11}$$

where a is the back-stress ratio and m and p'_0 are material parameters. Figure 4 illustrates the effect of parameters m and p_0 on the elliptic yield surface in the p'-q plane. Figure 4(a) implies that when p_0 is fixed, an increase of m inflates the elliptic yield surface. In Figure 4(b), the elliptic yield surface can be defined until $p' = p_0$ and the greater p'_0 makes the elliptic yield surface have the greater vertical size at the same p' value in the p'-q plane.

The gradients of the elliptic function f_e (equation (11)) to q and p' are written by

$$\frac{\partial f_e}{\partial q} = s, \tag{12}$$

$$\frac{\partial f_e}{\partial p'} = -sa - m\frac{(p_0 - 2p)}{2\sqrt{p(p_0 - p)}}. \tag{13}$$

Table 1: Calibrated parameters of the proposed yield surface for Toyoura sand.

Parameter	Value	Reference
C_g	850	[2, 22]
e_g	2.17	[2, 22]
n_g	0.45	[2, 22]
γ_{tl}	7×10^{-6}	[21]

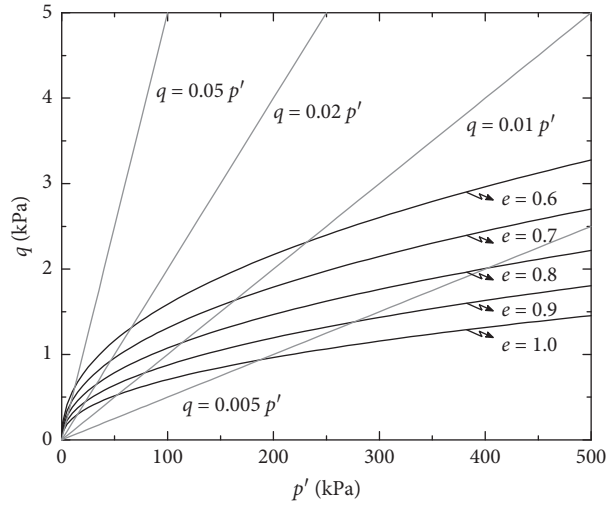

Figure 3: The calibrated yield surfaces (black lines) for Toyoura sand with various void ratio (0.6 to 1.0) compared with the linear yield surfaces (grey lines).

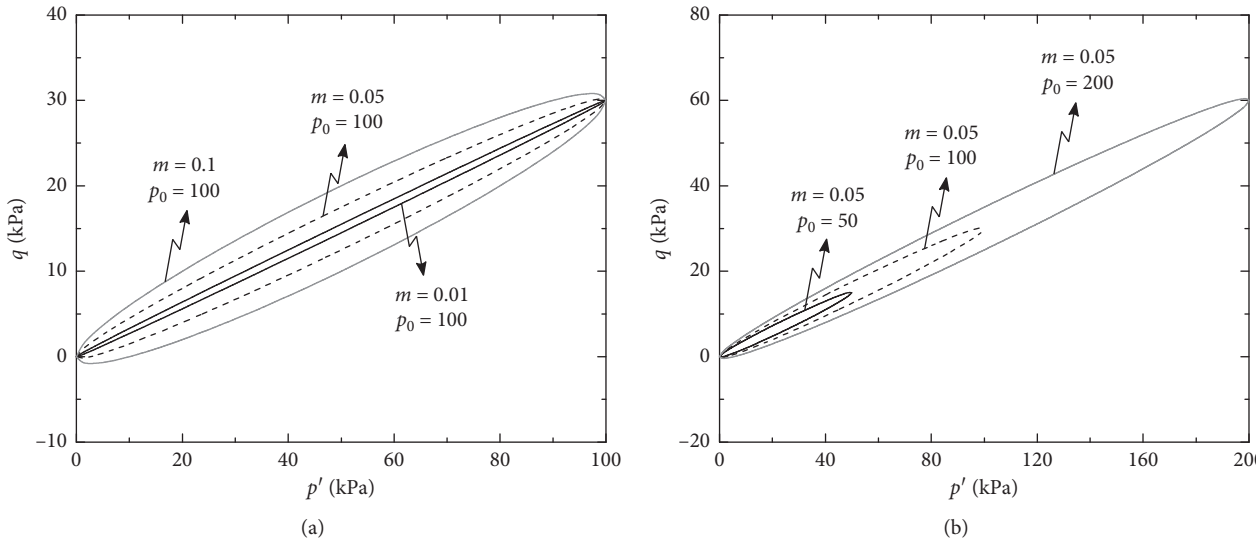

Figure 4: Dependency of an elliptical yield surface [23] on parameters (a) m and (b) p_0 when back-stress ratio $a = 0.3$.

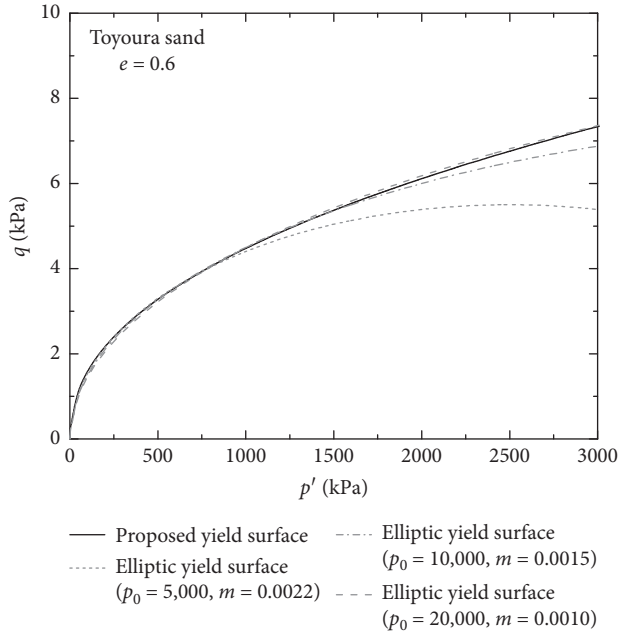

Figure 5: Determination of p_0 of the elliptic yield surface based on the proposed yield surface for Toyoura sand.

The gradient of f_e to q (equation (12)) is identical to the gradient of f (the proposed yield function) to q (equation (9)), whereas the gradient of f_e to p' (equation (13)) has a different second term from the gradient of f to p' (equation (10)). In equation (10), $\partial f/\partial p'$ is $-\infty$ at the origin ($p' = 0$) in the p'-q plane; as p' increases, $\partial f/\partial p'$ increases and it approaches to $-sa$ as p' goes to infinity; $\partial f_e/\partial p'$ is also $-\infty$ at the origin ($p' = 0$) in the p'-q plane; $\partial f_e/\partial p'$ approaches to $-sa$ as p' evolves to $(1/2)p_0$ from the origin; beyond this point ($p' = (1/2)p_0$), $\partial f_e/\partial p'$ starts to increases; at $p' = p_0$, $\partial f_e/\partial p'$ gets ∞; thus, for the elliptic yield surface to describe the proposed yield surface properly, the parameter p_0 should have great value so that the elliptic surface within $p' < p_0/2$ is close to the proposed yield surface.

Figure 5 shows how to determine p_0 of the elliptic yield surface corresponding to the proposed yield surface for Toyoura sand within the typical range (0 to 3000 kPa) of p'. In Figure 5, the grey lines are elliptic yield surfaces when $p_0 = 5{,}000$, 10,000, and 20,000 with m values that make the elliptic yield surfaces as close to the proposed yield surface as possible. Figure 5 shows that the greater p_0 enables the elliptic yield surface more closed to the proposed yield surface with a wide range of p'; this study sets p_0 as 20,000 for Toyoura sand. Figure 6 illustrates the proposed yield surfaces for Toyoura sand with void ratio

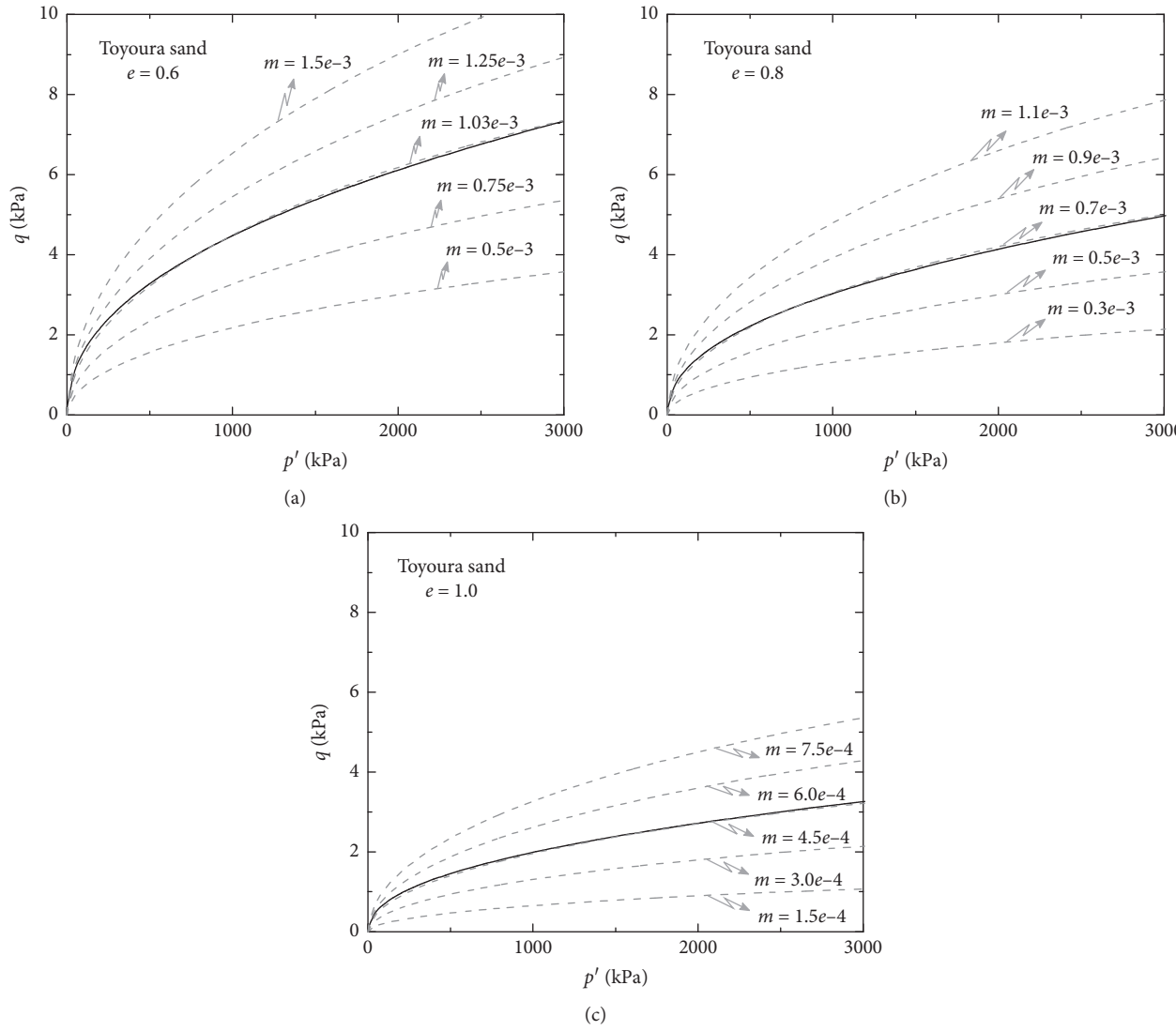

FIGURE 6: Determination of m of the elliptic yield surface (grey dot lines) based on the proposed yield surface (black solid lines) for Toyoura sand when p_0 is fixed as 20,000: (a) void ratio $e = 0.6$, (b) $e = 0.8$, and (c) $e = 1.0$.

$e = 0.6$, 0.8, and 1.0 overlapped the elliptical yield surfaces with various values of m and fixed value of p_0 (=20,000). According to Figure 6, for Toyoura sand specimens with $e = 0.6$, 0.8, and 1.0, the best matched elliptic yield surfaces have $m = 1.03e{-}3$, $0.7e{-}3$, and $4.5e{-}4$, respectively. For the undrained shearing, where the density (or void ratio) does not change, these calibrated elliptic yield surfaces (which have a simpler form than the proposed yield surface) can be adopted instead after proper determination of p_0 and m.

5. Conclusions

The present study proposes a rigorous mathematical expression of a yield function for sand based on the linear elastic threshold strain concept for the advanced constitutive modeling of sand. Conceptually, the linear elastic threshold strain in the strain space should correspond to the yield surface in the stress space. The new yield surface is formulated based on the linear elastic threshold strain that locates the yield points and empirical expression of the maximum shear modulus G_0, which represents the stress-strain relationship within the elastic range. The proposed yield function was calibrated for Toyoura sand. The calibration results show the following: (1) the size of yield surface depends on the void ratio of sand; the denser sand has the greater yield surface and (2) the proposed yield surfaces are nonlinear curves in the p'-q plane, whereas the linear lines have been adopted in the bounding surface modeling of sand.

This study also compared the elliptic yield surface with the proposed yield surface. The elliptic yield surface can describe the proposed yield surface accurately with adjustment of parameters and it can be used alternatives to the proposed yield surface under the undrained shearing where the void ratio (or density) of sand is fixed.

Data Availability

The data used to support the findings of this study are available from the corresponding author upon request.

Conflicts of Interest

The authors declare that they have no conflicts of interest.

Acknowledgments

The author gratefully acknowledges the financial support from the National Research Foundation of Korea (NRF) grant funded by the Korea government (MSIT) (no. NRF-2018R1A2B2002869).

References

[1] M. T. Manzari and Y. F. Dafalias, "A critical state two-surface plasticity model for sands," *Géotechnique*, vol. 47, no. 2, pp. 255–272, 1997.

[2] S. I. Woo and R. Salgado, "Bounding surface modeling of sand with consideration of fabric and its evolution during monotonic shearing," *International Journal of Solids and Structures*, vol. 63, pp. 277–288, 2015.

[3] Y. F. Dafalias and M. Taiebat, "SANISAND-Z: zero elastic range sand plasticity model," *Géotechnique*, vol. 66, no. 12, pp. 999–1013, 2016.

[4] D. Loukidis and R. Salgado, "Modeling sand response using two-surface plasticity," *Computers and Geotechnics*, vol. 36, no. 1-2, pp. 166–186, 2009.

[5] Y. F. Dafalias and M. T. Manzari, "Simple plasticity sand model accounting for fabric change effects," *Journal of Engineering Mechanics*, vol. 130, no. 6, pp. 622–634, 2004.

[6] K. I. Andrianopoulos, A. G. Papadimitriou, and G. D. Bouckovalas, "Explicit integration of bounding surface model for the analysis of earthquake soil liquefaction," *International Journal for Numerical and Analytical Methods in Geomechanics*, vol. 34, pp. 1586–1614, 2010.

[7] K. I. Andrianopoulos, A. G. Papadimitriou, and G. D. Bouckovalas, "Bounding surface plasticity model for the seismic liquefaction analysis of geostructures," *Soil Dynamics and Earthquake Engineering*, vol. 30, no. 10, pp. 895–911, 2010.

[8] J. A. H. Carraro, P. Bandini, and R. Salgado, "Liquefaction resistance of clean and nonplastic silty sands based on cone penetration resistance," *Journal of Geotechnical and Geoenvironmental Engineering*, vol. 129, no. 11, pp. 965–976, 2003.

[9] T. G. Murthy, D. Loukidis, J. A. H. Carraro, M. Prezzi, and R. Salgado, "Undrained monotonic response of clean and silty sands," *Géotechnique*, vol. 57, no. 3, pp. 273–288, 2007.

[10] R. Salgado, *The Engineering of Foundation*, McGraw-Hill, Pennsylvania Plaza, NY, USA, 2008.

[11] J. Mitchell and K. Soga, *Fundamentals of Soil Behavior*, J. Wiley & Sons, Hoboken, NJ, USA, 2005.

[12] A. Casagrande, "Characteristics of cohesionless soils affecting the stability of slopes and earth fills," *Journal of the Boston Society of Civil Engineers*, vol. 23, no. 1, pp. 13–32, 1936.

[13] A. Schofield and P. Wroth, *Critical State Soil Mechanics*, McGraw-Hill, Pennsylvania Plaza, NY, USA, 1968.

[14] P. Rowe, *The Stress-Dilatancy Relation for Static Equilibrium of an Assembly of Particles in Contact*, Proceedings of the Royal Society of London. Series A. Mathematical and Physical Sciences, vol. A269, pp. 500–527, 1962.

[15] G. De Josselin de Jong, "Rowe's stress-dilatancy relation based on friction," *Géotechnique*, vol. 26, no. 3, pp. 527–534, 1976.

[16] T. Chakraborty and R. Salgado, "Dilatancy and shear strength behavior of sand at low confining pressures," in *Proceedings of the 17th International Conference on Soil Mechanics and Geotechnical Engineering*, vol. 1, pp. 652–655, Washington, DC, USA, October 2009.

[17] J. Zhang and R. Salgado, "Stress-dilatancy relation for mohr-coulomb soils following a non-associated flow rule," *Géotechnique*, vol. 60, no. 3, pp. 223–226, 2010.

[18] M. D. Bolton, "The strength and dilatancy of sands," *Géotechnique*, vol. 36, no. 1, pp. 65–78, 1986.

[19] K. Been, M. G. Jefferies, and J. Hachey, "The critical state of sands," *Géotechnique*, vol. 41, no. 3, pp. 365–381, 1991.

[20] B. O. Hardin and F. E. Richart, "Elastic wave velocities in granular soils," *Journal of the Soil Mechanics and Foundations Division ASCE*, vol. 89, pp. 33–65, 1963.

[21] M. D. Bolton and S. Oztoprak, "Stiffness of sands through a laboratory test database," *Géotechnique*, vol. 63, no. 1, 2013.

[22] S. I. Woo, R. Salgado, and M. Prezzi, "Dilatancy-triggering surface for advanced constitutive modelling of sand," *Géotechnique Letters*, vol. 9, no. 2, pp. 136–141, 2019.

[23] M. Taiebat and Y. F. Dafalias, "Simple yield surface expressions appropriate for soil plasticity," *International Journal of Geomechanics*, vol. 10, no. 4, pp. 161–169, 2010.